Biochimica et Biophysica Acta 1813 (2011) 772–783

Contents lists available at ScienceDirect

Biochimica et Biophysica Acta

journal homepage: www.elsevier.com/locate/bbamcr

# ESeroS-GS modulates lipopolysaccharide-induced macrophage activation by impairing the assembly of TLR-4 complexes in lipid rafts

Wenjuan Duan [a,b,1], Juefei Zhou [a,c,1], Shen Zhang [a,d,1], Kai Zhao [a], Lijing Zhao [a,b], Kazumi Ogata [e], Takahiro Sakaue [e], Akitane Mori [f], Taotao Wei [a,*]

[a] National Laboratory of Biomacromolecules, Institute of Biophysics, Chinese Academy of Sciences, Beijing, China
[b] Graduate University of Chinese Academy of Science, Beijing, China
[c] Research Department of Bacterial Vaccine, Chengdu Institute of Biological Products, Chengdu, China
[d] Department of Laboratory Medicine, Huaihua Medical College, Huaihua, China
[e] Research Laboratory for Drug Discovery, Senju Pharmaceutical Co. Ltd., Osaka, Japan
[f] Okayama University School of Medicine, Okayama, Japan

ARTICLE INFO

*Article history:*
Received 31 August 2010
Received in revised form 13 January 2011
Accepted 18 January 2011
Available online 27 January 2011

*Keywords:*
ESeroS-GS
RAW264.7 macrophage
Lipopolysaccharide
Toll-like receptor-4
Lipid raft

ABSTRACT

The binding of lipopolysaccharides (LPS) to macrophages results in inflammatory responses. In extreme cases it can lead to endotoxic shock, often resulting in death. A broad range of antioxidants, including tocopherols, can reduce LPS activity *in vitro* and *in vivo*. To elucidate the underlying mechanisms of their action, we investigated the effect of the sodium salt of γ-L-glutamyl-S-[2-[[[3,4-dihydro-2,5,7,8-tetramethyl-2-(4,8,12-trimethyltridecyl)-2H-1-benzopyran-6-yl]oxy]carbonyl]-3-[[2-(1H-indol-3-yl)ethyl]amino]-3-oxopropyl]-L-cysteinylglycine (ESeroS-GS), a novel α-tocopherol derivative, on LPS-induced inflammation *in vitro* and *in vivo*. ESeroS-GS reduced the transcription of TNF-α, IL-1β, IL-6 and iNOS genes in a dose-dependent manner in RAW264.7 macrophages, and inhibited the release of these inflammatory factors. In addition, ESeroS-GS inhibited LPS-induced mortality in a mouse sepsis model. Electrophoretic mobility shift assays (EMSA) and reporter gene assays revealed that ESeroS-GS down-regulated the transcriptional activity of NF-κB. By analyzing the partitioning of CD14 and Toll-like receptor 4 (TLR-4) in cell membrane microdomains, we found that ESeroS-GS attenuates the binding of LPS to RAW264.7 cells via interfering with the relocation of CD14 and TLR-4 to lipid rafts, blocking the activation of interleukin-1 receptor-associated kinase 1 (IRAK-1), and inhibiting the consequent phosphorylation of TAK1 and IKKα/β, which together account for the suppression of NF-κB activation. Taken together, our data suggest that ESeroS-GS can modulate LPS signaling in macrophages by impairing TLR-4 complex assembly via a lipid raft dependent mechanism.



## 1. Introduction

Inflammation is a beneficial host response to foreign challenge or tissue injury, protecting the host against noxious materials and facilitating the restoration of tissue structure and function. Mononuclear phagocytes (monocytes and macrophages) exert key functions during this response which is vital for the recognition and elimination of invasive microbial pathogens [1–3]. Some bacterial components such as lipopolysaccharides (LPS; also termed endotoxin) can trigger the inflammatory response of mononuclear phagocytes. LPS is an integral structural component of the outer membrane of Gram-negative bacteria [4,5] and can be released during cell division, cell death, or as a result of antibiotic treatment against bacterial infection [6,7]. Upon its release, LPS is recognized by mononuclear phagocytes and activates innate immunity.

The onset of LPS activation of macrophages occurs when LPS (through its toxic entity, lipid A) binds to LPS binding protein (LBP), accelerating the binding of LPS to CD14, the primary receptor of LPS, which is expressed mainly in macrophages [8]. The LPS–CD14 complex initiates intracellular signaling by interacting with the transmembrane protein Toll-like receptor 4 (TLR-4) [9]. Assembly and activation of the TLR-4 complex initiates early processes of proinflammatory immune responses that help to strengthen the processes of innate and adaptive immunity, in which the nuclear factor κ-B (NF-κB) pathway plays many important roles. Activation of the NF-κB transcription factor is thought to act as a "master switch" for inflammation by regulating the transcription of genes involved in immunity and inflammation [10,11].

The NF-κB family of transcription factors includes homo- or heterodimers of p50, p52, p65 (RelA), c-Rel, and RelB. In the classical

* Corresponding author at: National Laboratory of Biomacromolecules, Institute of Biophysics, Chinese Academy of Sciences, 15 Datun Road, Chaoyang District, Beijing 100101, P. R. China. Tel.: +86 10 6488 8566; fax: +86 10 6487 1293.
*E-mail address:* weitt@moon.ibp.ac.cn (T. Wei).
[1] W. Duan, J. Zhou and S. Zhang contributed equally to this work.

0167-4889/$ – see front matter © 2011 Elsevier B.V. All rights reserved.
doi:10.1016/j.bbamcr.2011.01.019

activation pathway, activation of NF-κB is controlled by its inhibitory subunit, inhibitor of NF-κB (IκB), which prevents NF-κB subunits from leaving the cytosol. Upon activation by LPS and other agents, IκB is primarily phosphorylated by the IκB kinase (IKK) complex, resulting in the subsequent ubiquitination and degradation of IκB proteins via the proteosomal pathway. Degradation of IκB results in the release of NF-κB transcription factors, and free NF-κB is translocated to the nucleus where it binds to NF-κB binding sites in the promoter regions of target genes inducing their transcription [12]. The activation of NF-κB by LPS exposure in macrophages significantly enhances the secretion of proinflammatory cytokines such as tumor necrosis factor-α (TNF-α) and interleukin-1β (IL-1β) [13]. The expression of inflammation-related genes, such as inducible nitric oxide synthase (iNOS) [14] and cyclooxygenase-2 (COX-2) [15], is also induced.

Although proinflammatory cytokine secretion and inflammation-related gene expression in macrophages induced by LPS activation is essential for the development of the local inflammatory response, unbalanced production or overproduction of such proinflammatory factors (cytokines, nitric oxide, and prostaglandins) may lead to septic shock characterized by endothelial damage, loss of vascular tone, coagulopathy, and multiple system organ failure, often resulting in death [16]. Experimental models of sepsis have shown increased levels of TNF in the serum [17]. Hence, activation of macrophages must be tightly regulated, and identification of compounds with modulatory effects on activated macrophages represents an area of great relevance for these diseases.

It has been well documented that a broad range of antioxidants (including melatonin, flavonoids, polyphenols, and tocopherols) can abolish LPS activity and act as anti-inflammatory agents *in vitro* and *in vivo* [18–21]. α-Tocopherol inhibits the production of proinflammatory cytokines (TNF-α, macrophage inflammatory protein-2, and IL-1β) in neutrophils exposed to LPS, probably via a NF-κB-dependent mechanism [22]. *In vitro* treatment of human monocytes with 2,7,8-trimethyl-2-(β-carboxyethyl)-6-hydroxychroman (γ-CEHC; a metabolite of γ-tocopherol) inhibits LPS-induced degradation of IκB and JNK activation [23]. Dietary supplementation of mixed tocopherols in humans [23] or in mice [24] effectively inhibits the LPS-induced inflammatory response *in vivo*. These lines of evidence suggest that tocopherols might regulate the activation of macrophages and the subsequent production of proinflammatory factors via a redox-dependent NF-κB signaling pathway. However, the exact mechanisms are not yet clear.

Recently, it has been hypothesized that lipid raft microdomains may act as targets for antioxidants. The plasma membrane of cells was once believed to be homogeneous, but it is now clear that lipids in the cell membrane are organized in very small domains that are essential for cellular function. Lipid rafts are small membrane domains (less than 50 nm diameter) composed of glycosphingolipids and cholesterol, within which associated proteins are likely to be concentrated [25,26]. Although lipid rafts are known to exist, their physiological significance is not yet clear. One of the most widely appreciated roles of lipid rafts is in the recruitment and concentration of molecules involved in cellular signaling [27]. The accumulation of receptors and the downstream signal transduction machinery in lipid rafts seems to enhance signaling efficiency by providing a concentrating effect [28]. Thus, lipid raft microdomains can act as a platform for signal transduction [29–31].

Lipid rafts also play important roles in the immune system [32–34]. In macrophages, receptor molecules that are implicated in lipopolysaccharide (LPS)-cellular activation, such as CD14, heat shock protein (HSP) 70, HSP 90, chemokine receptor 4 (CXCR4), growth differentiation factor 5 (GDF5) and Toll-like receptor 4 (TLR-4), are present in microdomains following LPS stimulation [32]. CD14, the recognition receptor of LPS, is a GPI-anchored protein that does not have a cytoplasmic domain [8,35,36]. Following complex binding of LPS/LPB to CD14, the assembly of the TLR-4 complex, composed of CD14, TLR-4, myeloid differentiation protein 2, and HSP70, occurs in the lipid raft [37].

Since lipid raft microdomains act as platforms for macrophage activation, which might be regulated by antioxidants, the overall objective of the present study was to characterize the fundamental cellular mechanisms that link tocopherols and NF-κB activation in lipid rafts. We investigated the effect of the sodium salt of γ-L-glutamyl-S-[2-[[[3,4-dihydro-2,5,7,8-tetramethyl-2-(4,8,12-trimethyltridecyl)-2H-1-benzopyran-6-yl]oxy]carbonyl]-3-[[2-(1H-indol-3-yl)ethyl]amino]-3-oxopropyl]-L-cysteinylglycine (ESeroS-GS), a novel α-tocopherol derivative, on LPS-induced inflammation *in vitro* and *in vivo*, and hypothesized the underlying mechanisms.

## 2. Materials and methods

### 2.1. Chemicals and antibodies

The sodium salt of γ-L-glutamyl-S-[2-[[[3,4-dihydro-2,5,7,8-tetramethyl-2-(4,8,12-trimethyltridecyl)-2H-1-benzopyran-6-yl]oxy]carbonyl]-3-[[2-(1H-indol-3-yl)ethyl]amino]-3-oxopropyl]-L-cysteinylglycine (ESeroS-GS) was obtained from Senju Pharmaceutical Co. Ltd. (Osaka, Japan). Lipopolysaccharide (LPS; from *E. coli* 026:B6), FITC-LPS and α-tocopherol were purchased from Sigma-Aldrich (St. Louis, MO, USA). Dulbecco's modified Eagle's medium (DMEM), fetal bovine serum, cell culture supplements and Lipofectamine 2000™ were products of Invitrogen (Shanghai, China). Antibodies against phospho-TAK1 (Thr184/187), phospho-IKKα/β (Ser176/180), phospho-IκB-α (Ser32), phospho-IRAK-1 (Thr209), TAK1, IKKα/β, IκB-α, IRAK-1, CD14 and TLR-4 were purchased from Cell Signaling Technology (Danvers, MA, USA). Antibodies against iNOS, p65/RelA and p50 were purchased from BD Transduction Laboratories (San Jose, CA, USA). Other reagents were manufactured in China and were of analytical grade.

### 2.2. Cell culture and LPS exposure

RAW264.7 murine macrophages were obtained from the Chinese Type Culture Collection (CTCC, Shanghai, China) and were maintained in DMEM supplemented with 2 mM L-glutamine, 100 U/ml penicillin, 100 μg/ml streptomycin, and 10% heat-inactivated fetal bovine serum (v/v) [21]. Cells were incubated at 37 °C under a humidified atmosphere containing 5% $CO_2$/95% air. RAW264.7 macrophages (50% confluence) were stimulated with LPS (1 μg/ml) in serum-free DMEM for the times indicated. Cells were pretreated with ESeroS-GS (5, 20 or 50 μM) for 30 min before LPS exposure in some experiments, as indicated.

### 2.3. Mice experiments

Male C57BL/6J mice weighing 18–22 g were purchased from the Vital River Experimental Animal Center (Beijing, China) and used in accordance with the regulations approved by the Institutional Animal Care and Use Committee of Institute of Biophysics, Chinese Academy of Sciences (IACUC-IBP). Mice were randomly divided into 5 groups (12 mice per group). Group 1 mice were injected i.p. with saline; group 2 mice were injected i.p. with ESeroS-GS (100 mg/kg of body weight; dissolved in 0.85% NaCl, adjust to pH 7.4); group 3 mice were injected i.p. with a lethal dose of LPS (37.5 mg/kg); group 4 mice were injected i.p. with ESeroS-GS (100 mg/kg) 3 h before administration of LPS (37.5 mg/kg); group 5 mice were injected i.p. with LPS (37.5 mg/kg) for 3 h and then injected i.p. with ESeroS-GS (100 mg/kg). Survival was monitored every 3 h over the course of 120 h. Mantel–Haenszel log rank tests were performed and Kaplan–Meier survival curves were generated [20].

### 2.4. Immunodetection of cytokine secretion

RAW264.7 cells were incubated with or without ESeroS-GS for 30 min, and stimulated with LPS for 8 h. Cell culture supernatants were harvested to measure the levels of cytokines. In experiments used to determine serum levels of cytokines, mice were treated with LPS and/

or ESeroS-GS as outlined above, and blood was collected 1 h after the administration of LPS. The accumulation of the proinflammatory cytokines TNF-α, IL-1β and IL-6 in cell culture supernatants or sera was measured using sandwich ELISA kits (R&D Systems; Minneapolis, MN, USA) according to the manufacturer's protocols [38]. Data represent at least three independent experiments.

### 2.5. EPR detection of nitric oxide production

Direct evidence for the production of nitric oxide in LPS-activated macrophages was provided by EPR spin trapping using the ferrous diethyldithiocarbamate complex [$Fe^{2+}(DETC)_2$] as the spin trap. Although nitric oxide is a paramagnetic compound, it is EPR silent at room temperature in solution. However, when it is trapped with [$Fe^{2+}(DETC)_2$], the resulting complex [ON-$Fe^{2+}(DETC)_2$] is ESR-detectable at low temperature. Upon enrichment with organic solvents such as ethyl acetate, the hydrophilic [ON-$Fe^{2+}(DETC)_2$] complex can be detected at room temperature.

The experimental procedure used for nitric oxide detection has been described elsewhere [21]. Briefly, $2\times10^7$ RAW264.7 cells were stimulated with 1 μg/ml LPS for 12 h. The spin-trapping agent, containing 1 mM of $FeSO_4$, 5 mM of diethyldithiocarbamate sodium salt (DETC) and 5 mM of $Na_2S_2O_3$, was added to the activated macrophages, which were incubated at 37 °C for an additional 3 h. The paramagnetic [ON-$Fe^{2+}(DETC)_2$] complex was enriched by extraction with 200 μl ethyl acetate and detected with a Bruker ER-200 D-SRC EPR spectrometer under the following conditions: X-band; sweep width 400 G; microwave power 20 mW; 100 kHz modulation with amplitude 3.2 G; time constant 0.128 s.

### 2.6. RT-PCR detection of cytokine and iNOS mRNAs

RAW264.7 cells were stimulated with 1 μg/ml LPS for the lengths of time indicated. Total RNA was isolated from cells by using Uniq-10™ RNA purification kits (Sangon, Shanghai, China). RT-PCR analysis of TNF-α, IL-1β, IL-6, iNOS and GAPDH (as a housekeeping gene) mRNA levels was performed using AccessQuick™ RT-PCR kits (Promega, Shanghai, China) with the following primers: TNF-α forward: 5′-TTC TGT CTA CTG AAC TTC GGG GTG ATC GGT CC-3′, and reverse: 5′-GTA TGA GAT AGC AAA TCG GCT GAC GGT GTG GG-3′ (length of PCR product: 354bp); IL-1β forward: 5′-GAA GCT GTG GCA GCT ACC TAT GTC T-3′, and reverse: 5′-CTC TGC TTG TGA GGT GCT

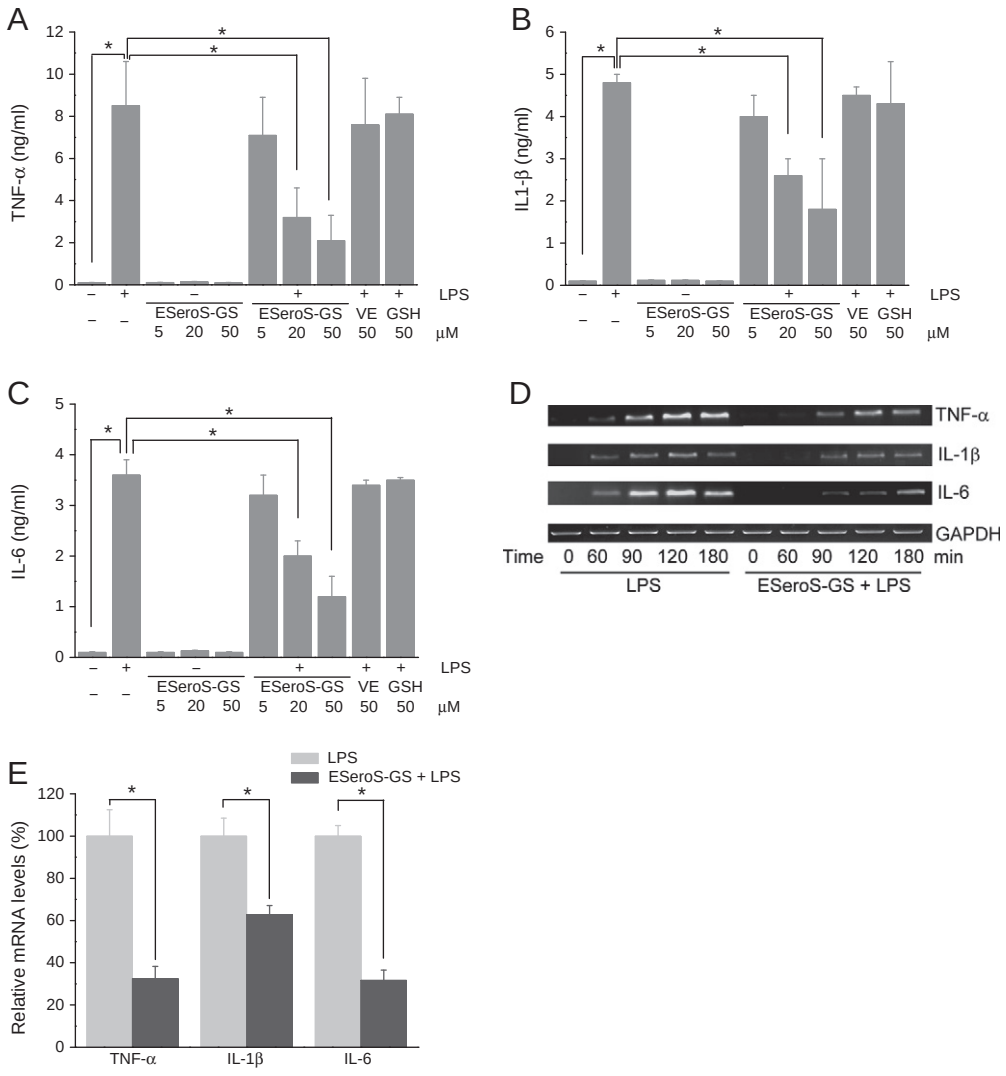


**Fig. 1.** ESeroS-GS inhibits the expression and production of cytokines. (A) TNF-α measurement. RAW264.7 cells were incubated with the indicated concentrations of ESeroS-GS for 30 min, and stimulated with 1 μg/ml LPS for 8 h. Cell culture supernatants were harvested and the accumulation of the proinflammatory cytokine TNF-α was measured using an R&D Systems sandwich ELISA kit. Values represent means ± SEM ($n=6$; *, $p<0.01$). (B) IL-1β measurement. (C) IL-6 measurement. (D) ESeroS-GS inhibits the mRNA expression of proinflammatory cytokines. RAW264.7 cells were incubated with 50 μM ESeroS-GS for 30 min, and stimulated with 1 μg/ml LPS for the lengths of time indicated. The mRNA levels of TNF-α, IL-1β and IL-6 were determined by RT-PCR. (E) Densitometric analysis of TNF-α, IL-1β and IL-6 mRNA levels normalized to GAPDH. RAW264.7 cells were incubated with 50 μM ESeroS-GS for 30 min, and stimulated with 1 μg/ml LPS for 180 min. Values represent means ± SEM ($n=3$; *, $p<0.01$).

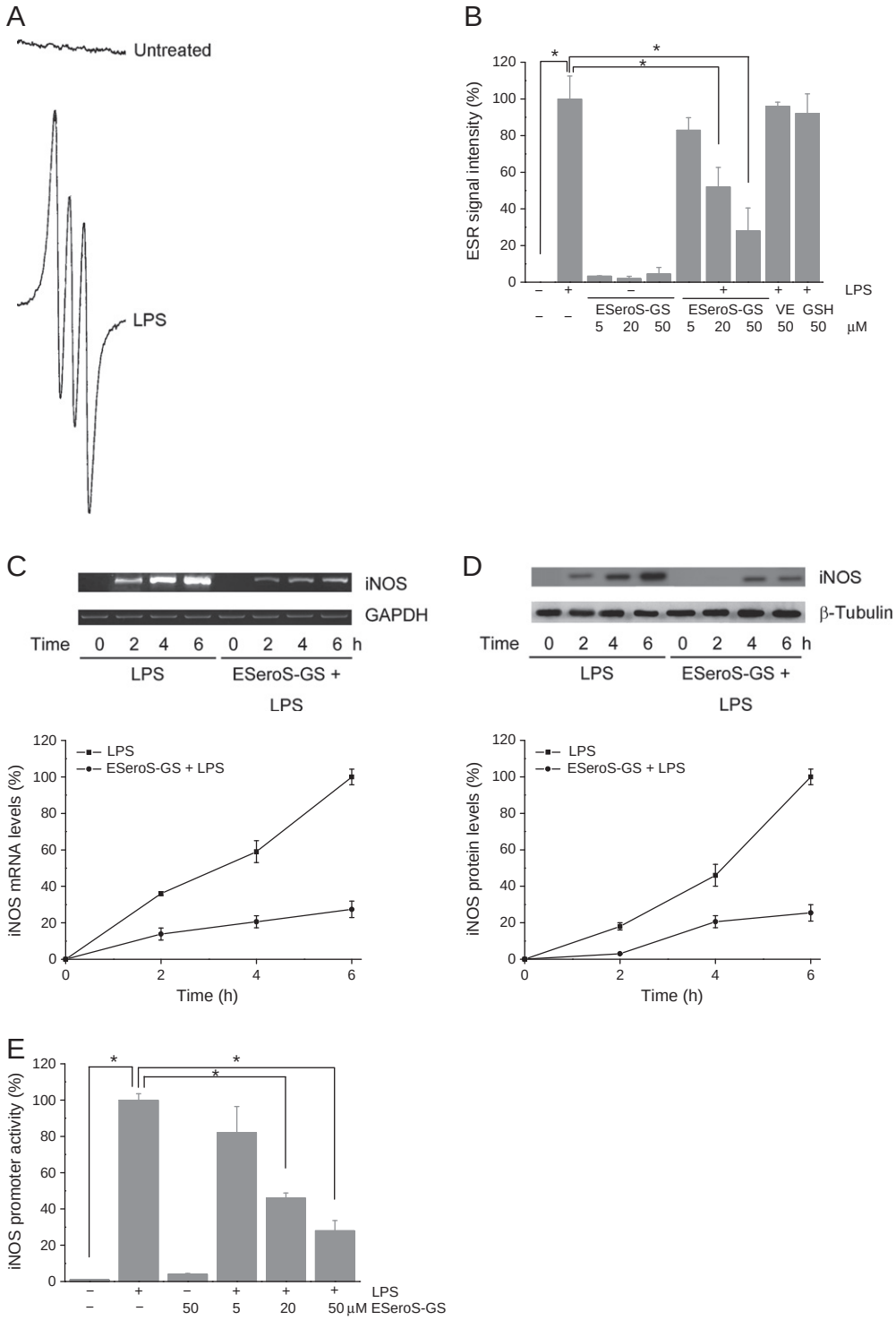


**Fig. 2.** ESeroS-GS inhibits the expression of iNOS and the production of NO. (A) Detection of NO production by EPR spin trapping. RAW264.7 cells were stimulated with 1 μg/ml LPS for 12 h. NO was trapped with $[Fe^{2+}(DETC)_2]$ and the paramagnetic $[ON\text{-}Fe^{2+}(DETC)_2]$ complex was enriched by extraction with ethyl acetate and detected with a Bruker ER-200 D-SRC EPR spectrometer. A three-line RPR spectrum could be observed in LPS-stimulated macrophages. (B) ESeroS-GS inhibits the production of NO. RAW264.7 cells were incubated with indicated concentrations of ESeroS-GS for 30 min, and stimulated with 1 μg/ml LPS for 12 h. The production of NO was detected by EPR spin trapping. Values represent means ± SEM ($n = 4$; *, $p < 0.01$). (C) ESeroS-GS inhibits the expression of iNOS mRNA. RAW264.7 cells were incubated with 50 μM ESeroS-GS for 30 min, and stimulated with 1 μg/ml LPS for the lengths of time indicated. The mRNA levels of iNOS were determined by RT-PCR. The upper panel shows representative results of RT-PCR, and the lower panel shows the densitometric analysis of iNOS mRNA normalized to GAPDH. Values represent means ± SEM ($n = 3$; *, $p < 0.01$). (D) ESeroS-GS inhibits the expression of iNOS protein. RAW264.7 cells were incubated with 50 μM ESeroS-GS for 30 min, and stimulated with 1 μg/ml LPS for the lengths of time indicated. Levels of iNOS protein were determined by Western blotting. The upper panel shows a representative Western blot, and the lower panel shows the densitometric analysis of iNOS protein normalized to β-tubulin. Values represent means ± SEM ($n = 3$; *, $p < 0.01$). (E) ESeroS-GS inhibits iNOS promoter activity. piNOS-LUC and pRL-TK-cotransfected cells were treated with the indicated concentrations of ESeroS-GS for 30 min before stimulation with 1 μg/ml LPS for 2 h. The firefly and Renilla luciferase activities in the cell lysates were detected, and the former activity was normalized to the latter activity. Values represent means ± SEM ($n = 3$; *, $p < 0.01$).

GAT GTA C-3′ (length of PCR product: 523bp); IL-6 forward: 5′-TTC CCT ACT TCA CAA GTC-3′, and reverse: 5′-ACT AGG TTT GCC GAG TAG-3′ (length of PCR product: 354bp); iNOS forward: 5′-GTG TTC CAC CAG GAG ATG TTG-3′, and reverse: 5′-CTC CTG CCC ACT GAG TTC GTC-3′ (length of PCR product: 576 bp); GAPDH forward: 5′-GAA GGG TGG GGC CAA AAG-3′, and reverse: 5′-GGA TGC AGG GAT GAT GTT CT-3′ (length of PCR product: 295 bp). PCR products were visualized by electrophoresis on 1.5% agarose gels stained with ethidium bromide.

### 2.7. Luciferase reporter assays

A firefly luciferase gene under the control of the iNOS promoter, piNOS-LUC (a generous gift from Dr. Jih-Pyang Wang, Graduate Institute of Pharmaceutical Chemistry, China Medical University), and a firefly luciferase gene under the control of four tandem copies of the consensus NF-κB site, pNF-κB-LUC (Clontech, Mountain View, CA, USA), were used to quantify iNOS promoter activity and NF-κB transcriptional activity, respectively [39]. A Renilla luciferase reporter under the control of the herpes simplex virus thymidine kinase promoter, pRL-TK (Promega), was used as an internal control to normalize the reporter gene activity. RAW264.7 cells were transiently transfected by Lipofectamine 2000™ (Invitrogen). Twenty-four hours later, the culture medium was replaced, and cells were treated with ESeroS-GS for 30 min followed by stimulation with LPS for 2 h. Then the cells were lysed, and the luciferase activity was determined by a Sirius luminometer using a dual-luciferase reporter assay (Promega) according to the manufacturer's instructions.

### 2.8. Electrophoretic mobility shift assays

Electrophoretic mobility shift assays (EMSA) were performed as described by Hou and coworkers [40], with minor modifications. In brief, biotinylated probes for NF-κB (5′-AGT TGA GGG GAC TTT CCC AGG C-3′ and 3′-TCA ACT CCC CTG AAA GGG TCC G-5′) were synthesized, and nuclear proteins were extracted from RAW264.7 cells using NE-PER nuclear protein extraction kits (Pierce, Beijing, China). EMSA assays of NF-κB activation were carried out using non-radioactive LightShift EMSA kits (Pierce) following the manufacturer's instructions. In brief, biotin-labeled DNA probes were incubated with nuclear extracts for 20 min in the presence of 0.05% Nonidet P-40 and 1 μg/μl dI-dC. Nuclear extracts were then subjected to 6% native PAGE and transferred to a nylon membrane. After cross-linking by UV light, the membrane was visualized by chemiluminescence and recorded with Kodak X-OMAT film.

### 2.9. Cell fractionation

Whole-cell lysates were prepared by lysing RAW264.7 cells in a buffer containing 1% Nonidet P-40, 0.25% sodium deoxycholate, 150 mM NaCl, 10 mM Tris, 1 mM EGTA, 1 mM $Na_3VO_4$, 1 mM NaF, 1 mM phenylmethylsulfonyl fluoride (PMSF), 1 μg/ml leupeptin, and 1 μg/ml aprotinin at 4 °C for 30 min [41].

Cytosolic and nuclear proteins were extracted from RAW264.7 cells as described previously [21]. Briefly, $10^7$ cells were lysed with 300 μl buffer A (0.2% Nonidet P-40, 10 mM Hepes, 10 mM KCl, 100 μM EDTA, 100 μM EGTA, 2 mM NaF, 1 mM PMSF, 1 μg/ml aprotinin and 1 μg/ml leupeptin) at 4 °C for 15 min. After centrifugation at 12,000 × *g* for 15 min, the supernatant containing cytosolic proteins was collected. The pellet was washed once with buffer A and then suspended in 100 μl of buffer B (20 mM Hepes, 390 mM NaCl, 1 mM EDTA, 1 mM EGTA, 2 mM NaF, and 2 mM phenylmethylsulfonyl fluoride). After centrifugation at 12,000 × g for 15 min, the supernatant was collected and used as nuclear proteins.

Lipid raft and non-raft fractions of RAW264.7 cells were prepared by sucrose gradient centrifugation [42]. Cells ($5 \times 10^7$) were lysed at 4 °C in 2 ml TNE buffer (25 mM Tris, 150 mM NaCl, 5 mM EDTA) containing 1% Triton X-100, 1 mM $Na_3VO_4$, 100 μM DTT, 200 μM PMSF, 1 μg/ml leupeptin, 1 μg/ml aprotinin, 50 mM NaF, 10 mM sodium pyrophosphate, 2.5 μg/ml pepstatin A, and 1 mM benzamidine. Lysates were then mixed with 2.5 ml 80% sucrose in TNE. Samples were then overlaid with 7 ml 35% sucrose in TNE followed by 3 ml 5% sucrose in TNE. Lysates were then spun for 18 h at 100,000 × *g* at 4°C. The gradient was then divided into 10 fractions, with fractions 2–4 representing the lipid raft fraction, and fractions 6–9 representing the non-raft fraction. Protein within the combined fractions was precipitated with trichloroacetic acid and then resuspended in 200 μl TNE.

### 2.10. Western blotting

Western blotting was performed using whole-cell lysates, cytosolic proteins, nuclear proteins, and lipid raft or non-raft fractions isolated from RAW264.7 cells. Samples were resolved by 10% SDS-PAGE, transferred to polyvinylidene fluoride (PVDF) membranes, and probed with primary antibodies. The membranes were incubated with peroxidase-conjugated secondary antibodies and visualized using a chemiluminescent substrate (ECL; GE Amersham Pharmacia, Beijing, China) and Kodak X-OMAT film (Rochester, NY, USA).

### 2.11. Analysis of LPS–FITC binding to RAW264.7 cells

RAW264.7 cells ($10^4$ cells/chamber) were plated in an 8-chamber Lab-Tek-chambered coverglass system (Nalgene Nunc, Rochester, NY, USA) and cultured overnight. Cells were pretreated with or without 50 μM of ESeroS-GS at 37 °C for 30 min, and then incubated with LPS–FITC (1 mg/ml) for 15 min. The cells were washed and covered with fresh medium. The uptake of LPS–FITC was analyzed using fluorescence confocal microscopy [43].

### 2.12. Data analysis

All data are expressed as the mean ± SD unless otherwise indicated. Differences between groups were compared by analysis of variance followed by post hoc Bonferroni tests to correct for multiple comparisons. Differences were considered to be statistically significant at $p<0.05$.

**Fig. 3.** ESeroS-GS inhibits the activation of NF-κB. (A) ESeroS-GS reduces the binding complex of NF-κB-DNA. RAW264.7 cells were treated with the indicated concentrations of ESeroS-GS for 30 min and then stimulated with 1 μg/ml LPS for 2 h. The binding complex of NF-κB-DNA was measured by electrophoretic mobility shift assay (EMSA) with NF-κB-specific biotin-labeled oligonucleotides. (B) ESeroS-GS decreases the NF-κB-dependent reporter gene expression. The pNF-κB-LUC and the pRL-TK-cotransfected cells were treated with the indicated concentrations of ESeroS-GS for 30 min before stimulation with 1 μg/ml LPS for 2 h. The firefly and Renilla luciferase activities in the cell lysates were detected, and the former activity was normalized to the latter activity. Values represent means ± SEM ($n=3$; *, $p<0.01$). (C) ESeroS-GS suppresses the phosphorylation and degradation of IκB-α. RAW264.7 cells were incubated with 50 μM ESeroS-GS for 30 min, and then stimulated with 1 μg/ml LPS for the lengths of time indicated. The levels of phosphorylated and total IκB-α were determined by Western blotting. The upper panel shows a representative Western blot, and the lower panel shows the densitometric analysis of phosphorylated and total IκB-α protein normalized to β-tubulin. Values represent means ± SEM ($n=3$; *, $p<0.01$). (D) ESeroS-GS inhibits the nuclear translocation of p65 and p50. RAW264.7 cells were incubated with 50 μM ESeroS-GS for 30 min, and then stimulated with 1 μg/ml LPS for the lengths of time indicated. The levels of nuclear p65 and p50 were determined by Western blotting. The upper panel shows a representative Western blot, and the lower panel shows the densitometric analysis of p65 and p50 protein normalized to lamin B. Values represent means ± SEM ($n=3$; *, $p<0.01$). (E) ESeroS-GS suppresses the phosphorylation of IKK and TAK1. RAW264.7 cells were incubated with 50 μM ESeroS-GS for 30 min, and then stimulated with 1 μg/ml LPS for 5 min. The levels of phosphorylated and total IKKα/β and TAK1 were determined by Western blotting. The upper panel shows a representative Western blot, and the lower panel shows the densitometric analysis of phosphorylated IKKα/β and TAK1 normalized to β-tubulin. Values represent means ± SEM ($n=3$; *, $p<0.01$). (F) ESeroS-GS suppresses the phosphorylation of IRAK-1. RAW264.7 cells were incubated with 50 μM ESeroS-GS for 30 min, and then stimulated with 1 μg/ml LPS for 5 min. Levels of phosphorylated and total IRAK-1 were determined by Western blotting. The upper panel shows representative results of Western blotting, and the lower panel shows the densitometric analysis of phosphorylated IRAK-1 normalized to β-tubulin. Values represent means ± SEM ($n=3$; *, $p<0.01$).

## 3. Results

### 3.1. ESeroS-GS inhibits the production of inflammatory cytokines in RAW264.7 macrophages

To test whether ESeroS-GS affected the release of proinflammatory cytokines in murine RAW264.7 macrophages, cells were pretreated with or without ESeroS-GS (5, 20 or 50 μM) for 30 min and then stimulated with LPS (1 μg/ml) for 8 h. We found that stimulation with LPS induced the release of TNF-α in RAW264.7 cells, while TNF-α was undetectable in cells left untreated (Fig. 1A). RAW264.7 cells pretreated with different doses of ESeroS-GS showed significant inhibition of LPS-induced TNF-α release at ESeroS-GS concentrations of 20 μM and higher (Fig. 1A). Similarly, the release of IL-1β and IL-6 in

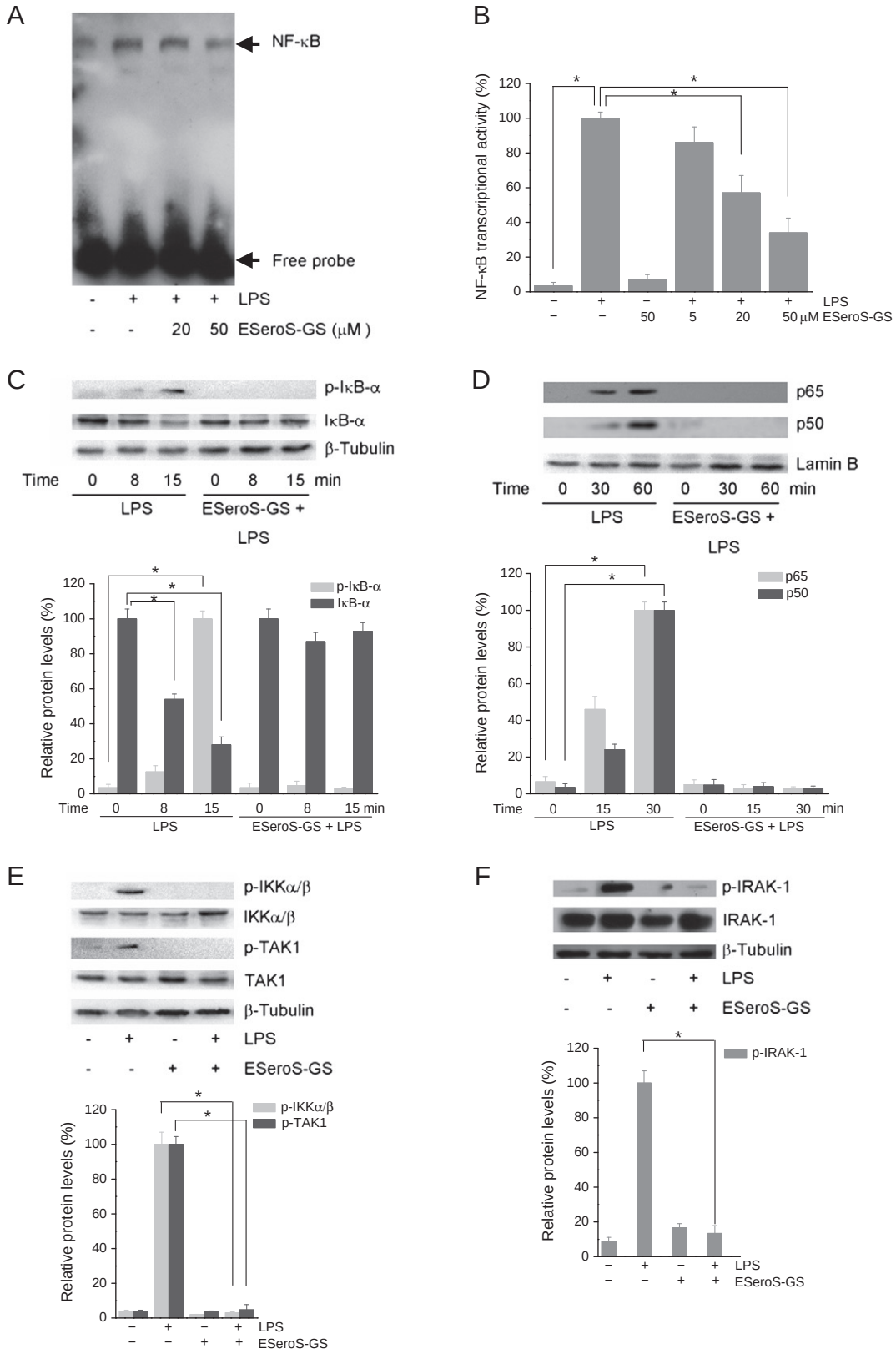

LPS-stimulated RAW264.7 cells could also be inhibited by pretreatment of cells with ESeroS-GS in a dose-dependent manner (Fig. 1B and C). Interestingly, neither α-tocopherol nor glutathione, the two precursors of ESeroS-GS, showed inhibitory effects on cytokine production, even at high concentrations.

To examine whether ESeroS-GS affected the release or the production of proinflammatory cytokines, we compared inflammatory cytokine mRNA levels. RT-PCR was performed on mRNA isolated from RAW264.7 cells stimulated with LPS for different lengths of time. Treatment with LPS alone induced a marked increase in the mRNA levels of TNF-α, IL-1β, and IL-6 compared with non-treated cells. Pretreatment with ESeroS-GS (50 μM) significantly reduced the levels of IL-1β, IL-6 and TNF-α mRNAs in LPS-stimulated cells (Fig. 1D). These results indicate that ESeroS-GS affects the transcript levels of several inflammatory cytokines.

### 3.2. ESeroS-GS down-regulates the expression of iNOS and decreases the production of NO in RAW264.7 macrophages

We measured LPS-induced production of NO in RAW264.7 cells by ESR spin trapping. A three-line ESR spectrum corresponding to the [ON-$Fe^{2+}$$(DETC)_2$] complex at $g=2.035$ was observed in RAW264.7 cells treated with LPS (1 μg/ml) for 12 h (Fig. 2A), suggesting that stimulated macrophages do generate nitric oxide. After pretreatment with 20 or 50 μM of ESeroS-GS, the signal intensity of the [ON-$Fe^{2+}$$(DETC)_2$] complex decreased significantly as shown in Fig. 2B, suggesting that ESeroS-GS inhibited NO production in RAW264.7 cells in a dose-dependent manner.

To investigate whether inhibition of NO production is due to a reduction in iNOS expression, we examined the effect of ESeroS-GS on the expression of the iNOS gene using RT-PCR and Western blotting. After exposure to 1 μg/ml LPS, the expression of iNOS was induced in a time-dependent manner as shown in Fig. 2C and D. Pretreatment with 50 μM of ESeroS-GS before LPS treatment significantly inhibited the expression of iNOS (Fig. 2C and D). In addition, ESeroS-GS decreased LPS-induced iNOS promoter activity in a dose-dependent manner as measured using a reporter gene assay (Fig. 2E). These results imply that ESeroS-GS down-regulates the expression of iNOS and decreases the production of NO, and that blockading the transcriptional process plays a critical role in the inhibition of iNOS expression.

### 3.3. ESeroS-GS attenuates LPS-induced NF-κB activation by suppressing IRAK/TAK/IKK phosphorylation

Since activation of NF-κB is responsible for the production of proinflammatory cytokines and NO upon LPS stimulation, we hypothesized that the NF-κB signaling pathway may be involved in ESeroS-GS-mediated inhibition of proinflammatory cytokines and iNOS expression. To demonstrate this, we determined the effect of ESeroS-GS on NF-κB transcriptional activity by electrophoretic mobility shift assays (EMSA) with NF-κB-specific biotin-labeled oligonucleotides, which were derived from NF-κB binding sequences in the murine iNOS promoter. RAW264.7 mouse macrophages were pretreated with or without ESeroS-GS for 30 min, stimulated with LPS for 2 h, and then subjected to EMSA. We found that LPS caused a marked increase in the binding of NF-κB to DNA (Fig. 3A, NF-κB-DNA in lane 2). ESeroS-GS at a final concentration of 50 μM significantly inhibited the binding of NF-κB to biotin-labeled DNA probes (Fig. 3A, lane 3), suggesting that the LPS-induced transcriptional activity of NF-κB was significantly reduced by treatment with ESeroS-GS. The expression of reporter genes in cells cotransfected with pNF-κB-LUC and pRL-TK was also analyzed. Consistent with the EMSA assay, the expression of NF-κB luciferase activity was inhibited in a concentration-dependent manner by ESeroS-GS (Fig. 3B). These results indicate that ESeroS-GS might suppress expression of proinflammatory cytokine and iNOS genes by blocking the binding of NF-κB to the promoter regions of these genes.

In quiescent macrophages, NF-κB is inactivated in the cytosol via binding to IκB. LPS initiates NF-κB activation via the phosphorylation and subsequent degradation of IκB, and NF-κB is then translocated to the nucleus where it binds to DNA [10]. Here, we investigated the effect of ESeroS-GS on IκB-α turnover in response to LPS stimulation. RAW264.7 cells were pretreated with 50 μM ESeroS-GS for 30 min and then treated with 1 μg/ml LPS for different lengths of time. LPS caused a rapid (~15 min after LPS stimulation) phosphorylation and degradation of IκB-α protein (Fig. 3C) in RAW264.7 cells which could be suppressed by pretreatment of cells with 50 μM of ESeroS-GS. These results suggest that ESeroS-GS might inhibit NF-κB activation by blocking LPS-induced IκB-α phosphorylation and degradation. To confirm this, we further examined the nuclear translocation of p65/Rel A and p50. In agreement with the above IκB-α degradation results, LPS resulted in marked p65/Rel A and p50 translocation from the cytosol to the nucleus, and ESeroS-GS (50 μM) significantly suppressed the nuclear translocation of p65/Rel A and p50 (Fig. 3D).

Since the phosphorylation of IκB proteins is regulated by the IκB kinases, IKKα/β, and phosphorylation of IKKα/β is further regulated by upstream factors such as TAK1, we next attempted to determine whether the inhibition effect of ESeroS-GS on LPS-induced NF-κB activation occurs through the TAK1/IKKα/β signaling pathway. Immunoblots showed that, in agreement with our results on the phosphorylation and degradation of IκB-α, LPS causes phosphorylation of TAK1 and IKKα/β (Fig. 3E), while ESeroS-GS pretreatment significantly decreases the LPS-stimulated phosphorylation of TAK1 and IKKα/β.

Upon binding of TLR-4 to LPS, the cytoplasmic region of TLR-4 recruits MyD88, which links TLR-4 to IRAK-1. IRAK-1 binds TRAF6 and then initiates a cascade of events leading to the phosphorylation of TAK1. We assayed the effects of ESeroS-GS on LPS-induced phosphorylation of IRAK-1. ESeroS-GS pretreatment significantly decreased LPS-stimulated phosphorylation of IRAK-1, as shown in Fig. 3F. The above data suggest that the IRAK-1/TAK1/IKKα/β signaling pathway is involved in the inhibition of NF-κB activation by ESeroS-GS.

### 3.4. ESeroS-GS inhibits the binding of LPS–FITC to RAW264.7 macrophages and attenuates LPS-induced lipid raft mobilization of CD14 and TLR-4

As the activation of macrophages by LPS starts when LPS binds to the cell membrane, we investigated the effects of ESeroS-GS on the binding of LPS to RAW264.7 macrophages. RAW264.7 cells were incubated with LPS–FITC (1 μg/ml) in the presence or absence of ESeroS-GS, and the uptake of FITC-labeled LPS was traced by confocal microscopy. As shown in Fig. 4A, ESeroS-GS inhibits LPS–FITC binding to the macrophages significantly.

Since CD14, the primary receptor of LPS which is mainly expressed in macrophages, is responsible for the binding and internalization of LPS [35], and since the interaction of the LPS–CD14 complex with the transmembrane protein TLR-4 initiates intracellular signaling [36,37], we examined whether ESeroS-GS inhibits LPS binding by CD14/TLR-4-related mechanisms. However, no changes in CD14 and TLR-4 expression were noted following ESeroS-GS pretreatment (Fig. 4B). Since the ligation of CD14 by LPS and the recruitment of multiple signaling molecules within the lipid rafts are the basis for cellular activation by LPS, we then investigated the effects of ESeroS-GS on the distribution of CD14 and TLR-4 in lipid raft fractions. The lipid raft and non-raft fractions were isolated from RAW264.7 cells by discontinuous sucrose density gradient centrifugation. As seen from Fig. 4C, the lipid rafts were mainly present in fraction 2 and, to a lesser extent, in fractions 1 and 3, as determined by the signal intensity of the lipid raft marker protein flotillin-1 and marker lipid ganglioside GM1. The distribution patterns of GM1,

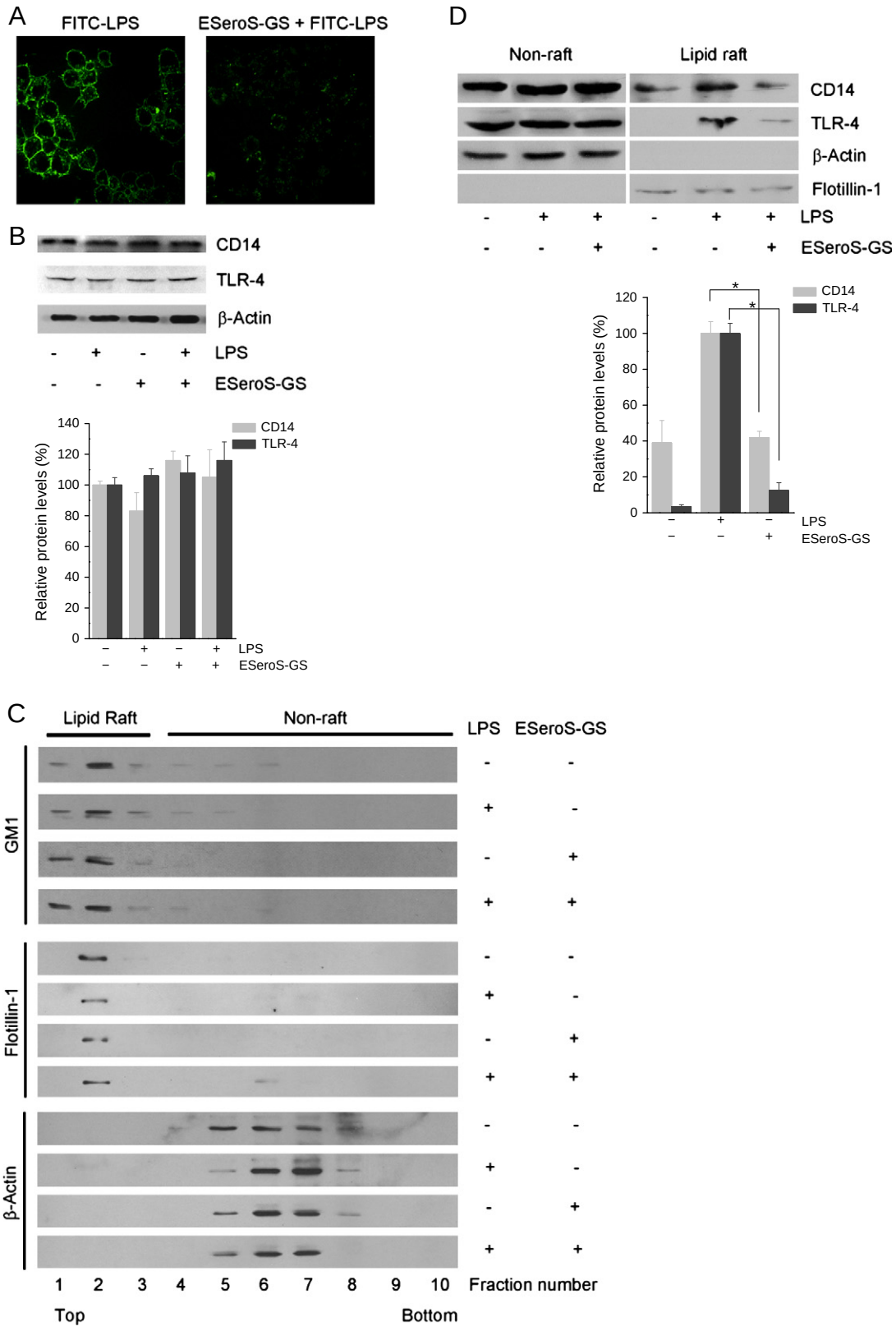


**Fig. 4.** ESeroS-GS inhibits LPS signaling by impairing the mobilization of CD14 and TLR-4 to lipid rafts. (A) ESeroS-GS inhibits the binding of LPS to RAW264.7 macrophages. RAW264.7 cells were incubated with 50 μM ESeroS-GS for 30 min, and then stimulated with 1 μg/ml FITC-LPS for 15 min. The binding of FITC-LPS to macrophages was observed by confocal microscopy. (B) ESeroS-GS has no effect on the expression of CD14 and TLR-4. RAW264.7 cells were incubated with 50 μM ESeroS-GS for 30 min and then stimulated with 1 μg/ml LPS for 5 min. The levels of CD14 and TLR-4 were determined by Western blotting. The upper panel shows representative results of Western blotting, and the lower panel shows the densitometric analysis of CD14 and TLR-4 normalized to β-actin. Values represent means ± SEM ($n = 3$; *, $p < 0.01$). (C) ESeroS-GS does not affect the buoyancy of lipid rafts. RAW264.7 cells were incubated with 50 μM ESeroS-GS for 30 min and then stimulated with 1 μg/ml LPS for 5 min. The lipid raft and non-raft fractions were isolated by discontinuous sucrose density gradient centrifugation and the distribution of GM1, flotillin-1 and β-actin in different fractions was analyzed by Western blotting. (D) ESeroS-GS inhibits the mobilization of CD14 and TLR-4 to lipid rafts. RAW264.7 cells were incubated with 50 μM ESeroS-GS for 30 min, and then stimulated with 1 μg/ml LPS for 5 min. The mobilization of CD14 and TLR-4 to lipid rafts was analyzed by Western blotting. The upper panel shows a representative Western blot, and the lower panel shows the densitometric analysis of CD14 and TLR-4 normalized to flotillin-1. Values represent means ± SEM ($n = 3$; *, $p < 0.01$).

flotillin-1 and β-actin were the same among cells treated with ESeroS-GS or LPS, indicating that ESeroS-GS and LPS do not affect the buoyancy of lipid rafts in general (Fig. 4C). Raft fractions (fractions 1–3) and non-raft fractions (fractions 4–10), defined according to flotillin-1 or GM1 distribution patterns, were combined separately and proteins were concentrated by TCA precipitation for detection of CD14 and TLR-4. The specificity of raft and non-raft fractions was further verified by the consistent detection of flotillin-1 only within the raft fraction and β-actin only within the non-raft fraction. As shown in Fig. 4D, relatively low CD14 and undetectable TLR-4 concentrations were present within the lipid raft prior to LPS exposure; however, exposure to LPS resulted in a significant increase in CD14 and TLR-4 protein within the lipid raft. This effect was attenuated by pretreatment with ESeroS-GS. These data suggest that the suppressive effects of ESeroS-GS on LPS-induced NF-κB activation might be related to the fact that ESeroS-GS interfered with LPS-induced redistribution of CD14 and TLR-4 to lipid raft fractions.

### 3.5. ESeroS-GS increases the life span of sepsis-bearing mice

Having shown that ESeroS-GS efficiently inhibits LPS stimulation of proinflammatory factors *in vitro*, we next investigated whether ESeroS-GS protects animals from LPS lethal toxicity in a sepsis model. C57BL/6J mice were injected with ESeroS-GS (100 mg/kg) or saline and then challenged i.p. with LPS. Pretreatment of mice with ESeroS-GS before LPS administration significantly attenuated the increase in serum cytokine levels (Fig. 5A–C).

Effects of ESeroS-GS on the life span of mice treated with a lethal dose of LPS were further investigated. All mice administered with LPS alone died in 48 h. However, pretreatment with ESeroS-GS before LPS injection increased survival to 66.7% at 48 h (Fig. 5D) and 58.3% at 120 h, and posttreatment with ESeroS-GS after LPS injection increased survival to 41.6% at 48 h (Fig. 5D) and 16.7% at 120 h, suggesting that ESeroS-GS increases life span of sepsis-bearing mice.

## 4. Discussion

LPS stimulation elicits a cascade leading to the activation of NF-κB and the production of proinflammatory molecules (including cytokines, nitric oxide, and prostaglandins). However, unbalanced or overproduction of such factors may lead to septic shock, often resulting in death [16]. Accordingly, inhibition of the LPS-stimulated signal transduction cascade might be a promising target for the treatment of sepsis. We here provide direct evidence that the sodium salt of γ-L-glutamyl-S-[2-[[[3,4-dihydro-2,5,7,8-tetramethyl-2-(4,8,12-trimethyltridecyl)-2H-1-benzopyran-6-yl]oxy]carbonyl]-3-[[2-(1H-indol-3-yl)ethyl]amino]-3-oxopropyl]-L-cysteinylglycine (ESeroS-GS), a novel α-tocopherol derivative, reduces the transcription of TNF-α, IL-1β, IL-6 and iNOS genes in LPS-stimulated RAW264.7 macrophages, and inhibits the release of these inflammatory factors (Figs. 1 and 2). In addition, we show that ESeroS-GS inhibits LPS-stimulated production of proinflammatory cytokines *in vivo* and increases the life span of sepsis-bearing mice (Fig. 5).

A broad range of antioxidants, including derivatives and analogs of tocopherols, could act as anti-inflammatory agents *in vitro* and *in vivo*, probably via a redox-dependent NF-κB signaling pathway [22–24]. We

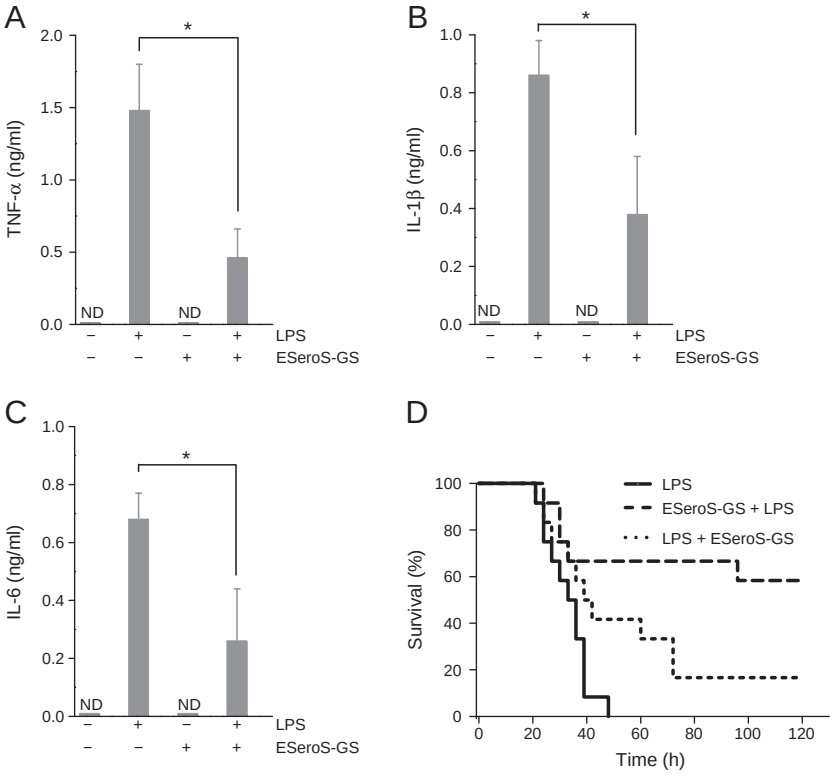


**Fig. 5.** ESeroS-GS *in vivo* affects serum proinflammatory cytokine concentration and increases life span of sepsis-bearing mice. (A) TNF-α measurement. C57BL/6J mice were injected with ESeroS-GS (100 mg/kg) or saline and then challenged i.p. with a lethal dose of LPS (37.5 mg/kg). Blood was collected 1 h after the administration of LPS. The accumulation of the proinflammatory cytokine TNF-α in serum samples was measured using an R&D Systems sandwich ELISA kit. Values represent means ± SEM ($n = 6$; *, $p < 0.01$). (B) IL-1β measurement. (C) IL-6 measurement. (D) ESeroS-GS increases life span of sepsis-bearing mice. Mice were randomly divided into 5 groups (12 mice per group). Group 1 mice were injected i.p. with saline; group 2 mice were injected i.p. with ESeroS-GS (100 mg/kg of body weight; dissolved in 0.85% NaCl, adjust to pH 7.4); group 3 mice were injected i.p. with a lethal dose of LPS (37.5 mg/kg); group 4 mice were injected i.p. with ESeroS-GS (100 mg/kg) 3 h before administration of LPS (37.5 mg/kg); group 5 mice were injected i.p. with LPS (37.5 mg/kg) for 3 h and then injected i.p. with ESeroS-GS (100 mg/kg). Survival was monitored every 3 h over the course of 120 h. Survival was monitored every 3 h over the course of 120 h. The Kaplan–Meier survival curve of group 3 (marked as LPS), group 4 (marked as ESeroS-GS + LPS) and group 5 (marked as LPS + ESeroS-GS) mice was shown.

therefore examined the effects of ESeroS-GS on LPS-induced NF-κB activation in RAW264.7 cells. The transcriptional activity of NF-κB was assessed in cells transiently transfected with a pNF-κB-LUC reporter construct containing four tandem copies of the NF-κB consensus sequence linked to the firefly luciferase gene. ESeroS-GS significantly inhibited the transcriptional activity of NF-κB (Fig. 3B). EMSA data also revealed that ESeroS-GS inhibited the binding complex of NF-κB-DNA present in the iNOS promoter (Fig. 3A). These findings are consistent with our previous report that ESeroS-GS inhibits iNOS expression in astrocytes via a NF-κB-dependent mechanism [41]. Western blotting results further revealed that the inhibition of NF-κB activation by ESeroS-GS might result from the suppression of IRAK-1, TAK1 and IκB-α phosphorylation (Fig. 3E), and subsequent inhibition of IκB-α degradation (Fig. 3C) and reduction of p65 and p50 nuclear translocation (Fig. 3D).

We then looked for the upstream molecule targeted by ESeroS-GS, by downregulating the LPS-stimulated activation of IRAK-1 cascades. ESeroS-GS effectively attenuated the binding and the internalization of FITC–LPS (Fig. 4A), as observed by laser confocal scanning microscopy; however, the expression of CD14 and TLR-4, the primary receptor of LPS in macrophages, was not affected by ESeroS-GS treatment (Fig. 4B). By analyzing the partitioning of CD14 and TLR-4 in different plasma membrane microdomains, we found that pretreatment of ESeroS-GS significantly alters the LPS-induced translocation of CD14 and TLR-4 into lipid rafts (Fig. 4D) without affecting the buoyancy of lipid rafts in general (Fig. 4C).

An important finding of this study is that ESeroS-GS significantly inhibits the activation of macrophages via lipid raft-dependent mechanisms. Although surface expression of CD14 and TLR-4 has not been shown to be affected by ESeroS-GS pretreatment, the LPS-induced translocation of CD14 and TLR-4 into lipid rafts was inhibited by ESeroS-GS, and thus the LPS-induced assembly of the TLR-4 complex in the lipid raft microdomains was altered.

Lipid rafts are mainly composed of sphingolipids and cholesterol (Fig. 6). The most prevalent component of sphingolipids in the cell membrane is sphingomyelin, which is composed of a highly hydrophobic ceramide moiety and a hydrophilic phosphorylcholine headgroup. The small cholesterol sterol-ring system and the ceramide moiety of sphingomyelin interact via hydrogen bonds and hydrophobic van der Waals interactions. Further hydrophilic interactions between sphingolipid headgroups promote the lateral association of sphingolipids and cholesterol. These interactions result in the separation of sphingolipids and cholesterol from other phospholipids in the cell membrane and thereby the formation of distinct microdomains. In these microdomains, cholesterol exerts a stabilizing role by filling the voids between the large and bulky sphingolipids. It is this cholesterol-sphingolipid interaction that determines the transition of these microdomains into a liquid-ordered or even gel-like phase, which is a unique characteristic of lipid rafts.

Lipid rafts are thought to dynamically organize cellular signaling events triggered by extracellular stimuli [25,26]. The dynamic remodeling of lipid rafts during proximal LPS signaling is believed to actively recruit non-raft proteins to rafts as well as to enrich selected raft-resident proteins [44]. Initial binding of LPS to CD14 results in the activation of acid sphingomyelinase and the consequent liberation of ceramide from the sphingomyelin [45]. Ceramide, which has a special ability to fuse membranes, appears to play important roles in the assembly of theTLR-4 complex [46]. Since treatment with antioxidants impairs sphingomyelinase activation and ceramide production [47], while ESeroS-GS inhibits macrophage activation via a lipid raft-dependent mechanism, we speculated whether ESeroS-GS acts as an antagonist of ceramide in the remodeling of lipid rafts. ESeroS-GS comprises α-tocopherol and glutathione linked to the core succinic acid, and its unique structure endows ESeroS-GS both hydrophilic and hydrophobic characteristics. However, we found that neither ESeroS-GS nor its precursors (α-tocopherol and glutathione) have apparent effects

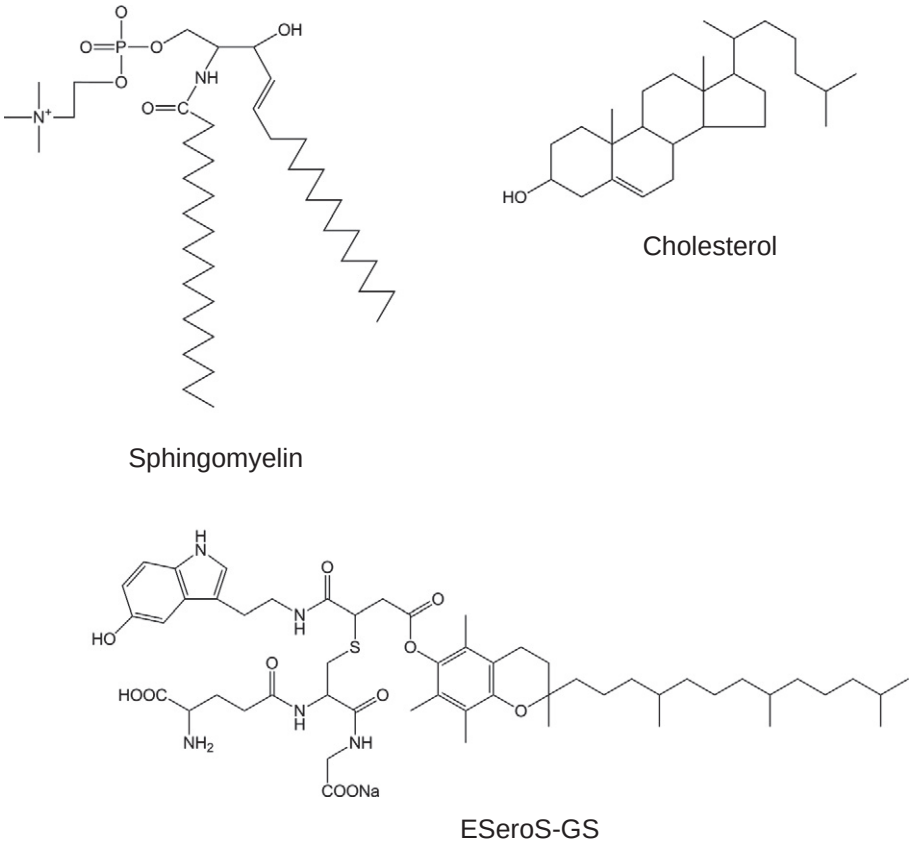


**Fig. 6.** Molecular structures of sphingomyelin, cholesterol, and ESeroS-GS.

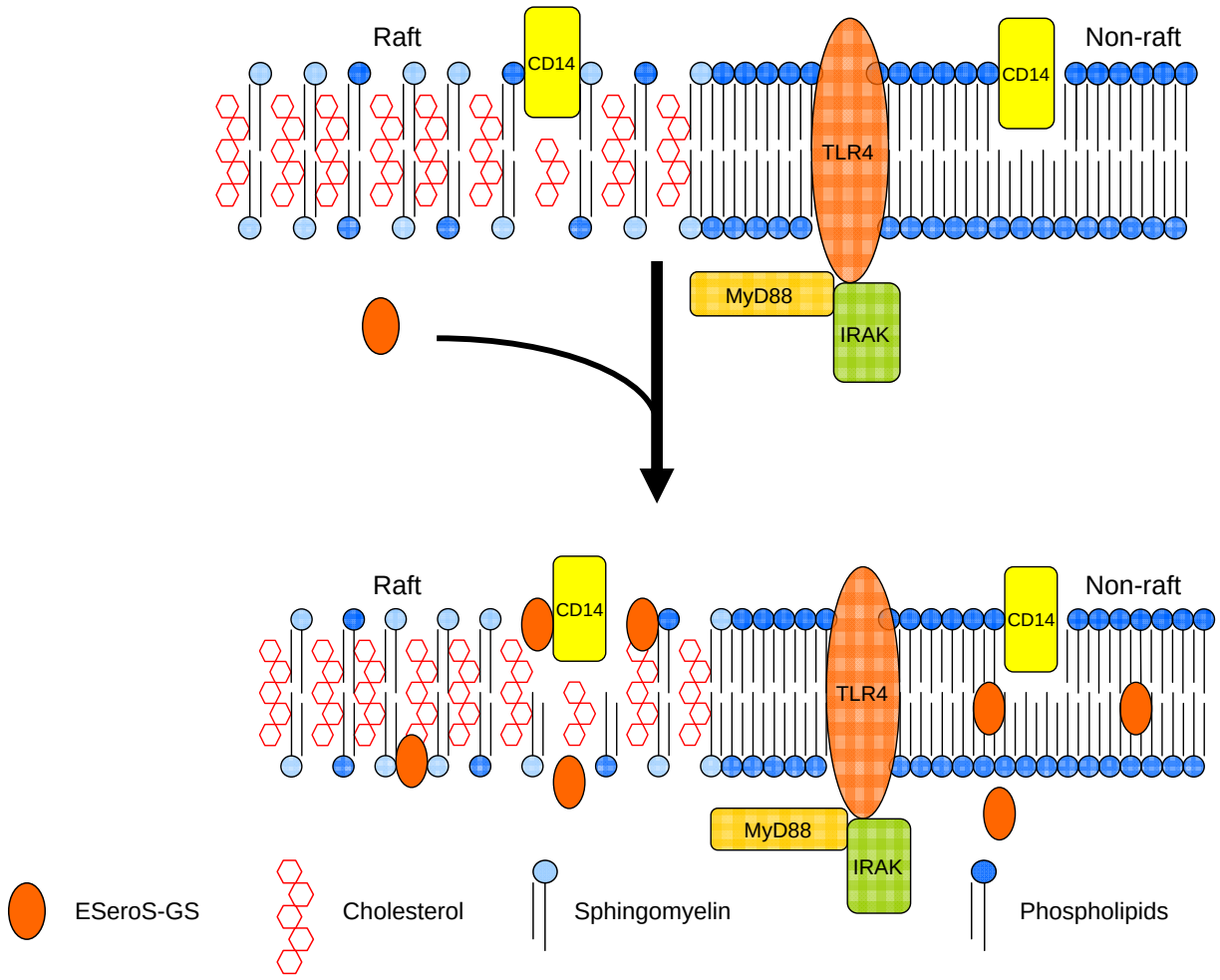


**Fig. 7.** Hypothesis of the effects of ESeroS-GS on lipid rafts.

on the activity of acid sphingomyelinase. The membrane fluidity in model membrane systems enriched with sphingomyelin and cholesterol was also not affected by ESeroS-GS, α-tocopherol or glutathione (data not shown). By analyzing the partitioning of lipid raft markers, we found that pretreatment of RAW264.7 macrophages with ESeroS-GS did not affect the buoyancy of lipid rafts in general (Fig. 4D). These data suggest that ESeroS-GS might not affect the lipid raft directly (Fig. 7)..

It has been reported that lipid rafts are targets of several antioxidants, including (−)-epigallocatechin gallate (EGCG; a major component of green tea polyphenols) [48,49], quercetin [50], resveratrol [51], and tocopherol [52]. However, the underlying mechanisms by which these antioxidants affect the lipid raft remains an open question. Plant flavonoids can influence the appearance and development of rafts or raft-like membrane domains in cellular membranes, and thus influence the lateral diffusion of lipid molecules [53]. One recent hypothesis is that α-tocopherol partitions into domains that are enriched in highly disordered polyunsaturated phospholipid domains. These highly disordered domains which are depleted in cholesterol are analogous, but organizationally antithetical, to lipid rafts [54]. Domains that are enriched in either sphingolipids and cholesterol (lipid rafts) or polyunsaturated phospholipids (disordered domains) are both targets of redox signaling [55], especially in macrophages [50,56].

In conclusion, we have demonstrated that ESeroS-GS can protect mice from LPS-induced lethality. Moreover, ESeroS-GS inhibits the production of proinflammatory factors *in vivo* and *in vitro*. Our findings provide novel insights into the molecular mechanisms by which ESeroS-GS regulates inflammation and show that ESeroS-GS functions by regulating NF-κB activity through the suppression of lipid raft-dependent assembly of TLR-4 complexes. How the novel antioxidant ESeroS-GS disrupts the assembly of the TLR-4 complex in lipid rafts remains unclear, and further investigation is required to determine the precise site of ESeroS-GS action in the dynamic remodeling of lipid rafts.

## Acknowledgements

This work was supported by grants from the National Natural Science Foundation of China (Grants 30770492, 30900246 and 31070736) and the National Basic Research Program of China (Grant 2010CB833700). We would like to thank Dr. Jih-Pyang Wang (China Medical University) for kindly providing the piNOS-LUC vector, and Profs. Fuyu Yang and Wenjuan Xin (Institute of Biophysics, CAS) for valuable suggestions and discussions. The authors are also indebted to Wenmin Zhong, Joy Fleming, Xingyu Zhao, Wei Li and Pengtao Jiang (Institute of Biophysics, CAS) for their technical assistance.

## References

[1] S. Greenberg, S. Grinstein, Phagocytosis and innate immunity, Curr. Opin. Immunol. 14 (2002) 136–145.
[2] X. Zhang, D.M. Mosser, Macrophage activation by endogenous danger signals, J. Pathol. 214 (2008) 161–178.
[3] R. Medzhitov, C.A. Janeway Jr., Decoding the patterns of self and nonself by the innate immune system, Science 296 (2002) 298–300.
[4] C.R. Raetz, C. Whitfield, Lipopolysaccharide endotoxins, Annu. Rev. Biochem. 71 (2002) 635–700.
[5] M.P. Bos, J. Tommassen, Biogenesis of the Gram-negative bacterial outer membrane, Curr. Opin. Microbiol. 7 (2004) 610–616.

[6] D.A. Hopkin, Frapper fort ou frapper doucement: a gram-negative dilemma, Lancet 2 (1978) 1193–1194.
[7] R.E. Hancock, M.G. Scott, The role of antimicrobial peptides in animal defenses, Proc. Natl Acad. Sci. USA 97 (2000) 8856–8861.
[8] D. Heumann, R. Lauener, B. Ryffel, The dual role of LBP and CD14 in response to Gram-negative bacteria or Gram-negative compounds, J. Endotoxin Res. 9 (2003) 381–384.
[9] S. Akira, Toll-like receptors and innate immunity, Adv. Immunol. 78 (2001) 1–56.
[10] P. Viatour, M.P. Merville, V. Bours, A. Chariot, Phosphorylation of NF-kappaB and IkappaB proteins: implications in cancer and inflammation, Trends Biochem. Sci. 30 (2005) 43–52.
[11] S. Akira, S. Uematsu, O. Takeuchi, Pathogen recognition and innate immunity, Cell 124 (2006) 783–801.
[12] S. Beinke, S.C. Ley, Functions of NF-kappaB1 and NF-kappaB2 in immune cell biology, Biochem. J. 382 (2004) 393–409.
[13] E.T. Rietschel, H. Brade, O. Holst, L. Brade, S. Muller-Loennies, U. Mamat, U. Zahringer, F. Beckmann, U. Seydel, K. Brandenburg, A.J. Ulmer, T. Mattern, H. Heine, J. Schletter, H. Loppnow, U. Schonbeck, H.D. Flad, S. Hauschildt, U.F. Schade, F. Di Padova, S. Kusumoto, R.R. Schumann, Bacterial endotoxin: chemical constitution, biological recognition, host response, and immunological detoxification, Curr. Top. Microbiol. Immunol. 216 (1996) 39–81.
[14] Q.W. Xie, R. Whisnant, C. Nathan, Promoter of the mouse gene encoding calcium-independent nitric oxide synthase confers inducibility by interferon gamma and bacterial lipopolysaccharide, J. Exp. Med. 177 (1993) 1779–1784.
[15] R.M. Silver, S.S. Edwin, M.S. Trautman, D.L. Simmons, D.W. Branch, D.J. Dudley, M.D. Mitchell, Bacterial lipopolysaccharide-mediated fetal death. Production of a newly recognized form of inducible cyclooxygenase (COX-2) in murine decidua in response to lipopolysaccharide, J. Clin. Invest. 95 (1995) 725–731.
[16] J. Cohen, The immunopathogenesis of sepsis, Nature 420 (2002) 885–891.
[17] K.J. Tracey, A. Cerami, Tumor necrosis factor, other cytokines and disease, Annu. Rev. Cell Biol. 9 (1993) 317–343.
[18] Q. Chen, D.W. Powell, M.J. Rane, S. Singh, W. Butt, J.B. Klein, K.R. McLeish, Akt phosphorylates p47phox and mediates respiratory burst activity in human neutrophils, J. Immunol. 170 (2003) 5302–5308.
[19] J. Leiro, E. Alvarez, J.A. Arranz, R. Laguna, E. Uriarte, F. Orallo, Effects of cis-resveratrol on inflammatory murine macrophages: antioxidant activity and down-regulation of inflammatory genes, J. Leukoc. Biol. 75 (2004) 1156–1165.
[20] C. Nicholas, S. Batra, M.A. Vargo, O.H. Voss, M.A. Gavrilin, M.D. Wewers, D.C. Guttridge, E. Grotewold, A.I. Doseff, Apigenin blocks lipopolysaccharide-induced lethality in vivo and proinflammatory cytokines expression by inactivating NF-kappaB through the suppression of p65 phosphorylation, J. Immunol. 179 (2007) 7121–7127.
[21] S. Zhang, W. Li, Q. Gao, T. Wei, Effect of melatonin on the generation of nitric oxide in murine macrophages, Eur. J. Pharmacol. 501 (2004) 25–30.
[22] K. Asehnoune, D. Strassheim, S. Mitra, J.Y. Kim, E. Abraham, Involvement of reactive oxygen species in Toll-like receptor 4-dependent activation of NF-kappa B, J. Immunol. 172 (2004) 2522–2529.
[23] J. Wiser, N.E. Alexis, Q. Jiang, W. Wu, C. Robinette, R. Roubey, D.B. Peden, In vivo gamma-tocopherol supplementation decreases systemic oxidative stress and cytokine responses of human monocytes in normal and asthmatic subjects, Free Radic. Biol. Med. 45 (2008) 40–49.
[24] E.G. Novoselova, S.M. Lunin, T.V. Novoselova, M.O. Khrenov, O.V. Glushkova, N.V. Avkhacheva, V.G. Safronova, E.E. Fesenko, Naturally occurring antioxidant nutrients reduce inflammatory response in mice, Eur. J. Pharmacol. 615 (2009) 234–240.
[25] K. Simons, E. Ikonen, Functional rafts in cell membranes, Nature 387 (1997) 569–572.
[26] D.A. Brown, E. London, Functions of lipid rafts in biological membranes, Annu. Rev. Cell Dev. Biol. 14 (1998) 111–136.
[27] A. Pralle, P. Keller, E.L. Florin, K. Simons, J.K. Horber, Sphingolipid-cholesterol rafts diffuse as small entities in the plasma membrane of mammalian cells, J. Cell Biol. 148 (2000) 997–1008.
[28] G. Vereb, J. Matko, G. Vamosi, S.M. Ibrahim, E. Magyar, S. Varga, J. Szollosi, A. Jenei, R. Gaspar Jr., T.A. Waldmann, S. Damjanovich, Cholesterol-dependent clustering of IL-2Ralpha and its colocalization with HLA and CD48 on T lymphoma cells suggest their functional association with lipid rafts, Proc. Natl. Acad. Sci. USA 97 (2000) 6013–6018.
[29] K. Simons, D. Toomre, Lipid rafts and signal transduction, Nat. Rev. Mol. Cell Biol. 1 (2000) 31–39.
[30] L.J. Pike, Lipid rafts: bringing order to chaos, J. Lipid Res. 44 (2003) 655–667.
[31] J.A. Allen, R.A. Halverson-Tamboli, M.M. Rasenick, Lipid raft microdomains and neurotransmitter signalling, Nat. Rev. Neurosci. 8 (2007) 128–140.
[32] M. Triantafilou, K. Miyake, D.T. Golenbock, K. Triantafilou, Mediators of innate immune recognition of bacteria concentrate in lipid rafts and facilitate lipopolysaccharide-induced cell activation, J. Cell Sci. 115 (2002) 2603–2611.
[33] M. Dykstra, A. Cherukuri, H.W. Sohn, S.J. Tzeng, S.K. Pierce, Location is everything: lipid rafts and immune cell signaling, Annu. Rev. Immunol. 21 (2003) 457–481.
[34] J. Riethmuller, A. Riehle, H. Grassme, E. Gulbins, Membrane rafts in host-pathogen interactions, Biochim. Biophys. Acta 1758 (2006) 2139–2147.
[35] C. Schutt, Cd14, Int. J. Biochem. Cell Biol. 31 (1999) 545–549.
[36] G. Schmitz, E. Orso, CD14 signalling in lipid rafts: new ligands and co-receptors, Curr. Opin. Lipidol. 13 (2002) 513–521.
[37] M. Triantafilou, K. Triantafilou, Lipopolysaccharide recognition: CD14, TLRs and the LPS-activation cluster, Trends Immunol. 23 (2002) 301–304.
[38] T.L. Adair-Kirk, J.J. Atkinson, D.G. Kelley, R.H. Arch, J.H. Miner, R.M. Senior, A chemotactic peptide from laminin alpha 5 functions as a regulator of inflammatory immune responses via TNF alpha-mediated signaling, J. Immunol. 174 (2005) 1621–1629.
[39] L.T. Tsao, P.S. Tsai, R.H. Lin, L.J. Huang, S.C. Kuo, J.P. Wang, Inhibition of lipopolysaccharide-induced expression of inducible nitric oxide synthase by phenolic (3E)-4-(2-hydroxyphenyl)but-3-en-2-one in RAW 264.7 macrophages, Biochem. Pharmacol. 70 (2005) 618–626.
[40] D.X. Hou, D. Luo, S. Tanigawa, F. Hashimoto, T. Uto, S. Masuzaki, M. Fujii, Y. Sakata, Prodelphinidin B-4 3′-O-gallate, a tea polyphenol, is involved in the inhibition of COX-2 and iNOS via the downregulation of TAK1-NF-kappaB pathway, Biochem. Pharmacol. 74 (2007) 742–751.
[41] T. Wei, X. Zhao, J. Hou, K. Ogata, T. Sakaue, A. Mori, W. Xin, The antioxidant ESeroS-GS inhibits NO production and prevents oxidative stress in astrocytes, Biochem. Pharmacol. 66 (2003) 83–91.
[42] J. Cuschieri, J. Billigren, R.V. Maier, Endotoxin tolerance attenuates LPS-induced TLR4 mobilization to lipid rafts: a condition reversed by PKC activation, J. Leukoc. Biol. 80 (2006) 1289–1297.
[43] Y. Rosenfeld, N. Papo, Y. Shai, Endotoxin (lipopolysaccharide) neutralization by innate immunity host-defense peptides. Peptide properties and plausible modes of action, J. Biol. Chem. 281 (2006) 1636–1643.
[44] S. Dhungana, B.A. Merrick, K.B. Tomer, M.B. Fessler, Quantitative proteomics analysis of macrophage rafts reveals compartmentalized activation of the proteasome and of proteasome-mediated ERK activation in response to lipopolysaccharide, Mol. Cell. Proteomics 8 (2009) 201–213.
[45] J. Cuschieri, R.V. Maier, Oxidative stress, lipid rafts, and macrophage reprogramming, Antioxid. Redox Signal. 9 (2007) 1485–1497.
[46] J. Cuschieri, E. Bulger, J. Billgrin, I. Garcia, R.V. Maier, Acid sphingomyelinase is required for lipid Raft TLR4 complex formation, Surg. Infect. (Larchmt) 8 (2007) 91–106.
[47] X. Li, K.A. Becker, Y. Zhang, Ceramide in redox signaling and cardiovascular diseases, Cell. Physiol. Biochem. 26 (2010) 41–48.
[48] S. Adachi, T. Nagao, H.I. Ingolfsson, F.R. Maxfield, O.S. Andersen, L. Kopelovich, I.B. Weinstein, The inhibitory effect of (−)-epigallocatechin gallate on activation of the epidermal growth factor receptor is associated with altered lipid order in HT29 colon cancer cells, Cancer Res. 67 (2007) 6493–6501.
[49] S.K. Patra, F. Rizzi, A. Silva, D.O. Rugina, S. Bettuzzi, Molecular targets of (−)-epigallocatechin-3-gallate (EGCG): specificity and interaction with membrane lipid rafts, J. Physiol. Pharmacol. 59 (Suppl 9) (2008) 217–235.
[50] T.K. Kao, Y.C. Ou, S.L. Raung, C.Y. Lai, S.L. Liao, C.J. Chen, Inhibition of nitric oxide production by quercetin in endotoxin/cytokine-stimulated microglia, Life Sci. 86 (2010) 315–321.
[51] C.M. Klinge, N.S. Wickramasinghe, M.M. Ivanova, S.M. Dougherty, Resveratrol stimulates nitric oxide production by increasing estrogen receptor alpha-Src-caveolin-1 interaction and phosphorylation in human umbilical vein endothelial cells, FASEB J. 22 (2008) 2185–2197.
[52] J. Cuschieri, E. Bulger, J. Biligren, I. Garcia, R.V. Maier, Vitamin E inhibits endotoxin-mediated transport of phosphatases to lipid rafts, Shock 27 (2007) 19–24.
[53] Y.S. Tarahovsky, E.N. Muzafarov, Y.A. Kim, Rafts making and rafts braking: how plant flavonoids may control membrane heterogeneity, Mol. Cell. Biochem. 314 (2008) 65–71.
[54] J. Atkinson, T. Harroun, S.R. Wassall, W. Stillwell, J. Katsaras, The location and behavior of alpha-tocopherol in membranes, Mol. Nutr. Food Res. 54 (2010) 641–651.
[55] P.L. Li, E. Gulbins, Lipid rafts and redox signaling, Antioxid. Redox Signal. 9 (2007) 1411–1415.
[56] G. Schmitz, M. Grandl, Role of redox regulation and lipid rafts in macrophages during Ox-LDL-mediated foam cell formation, Antioxid. Redox Signal. 9 (2007) 1499–1518.